Electronic states on InP(110)–Sb(1 ML)

G P Srivastava and R P Martin

Semiconductor Physics Group, Physics Department, University of Exeter, Exeter EX4 4QL, UK

Abstract. A self-consistent calculation has been made, using non-local norm-conserving pseudopotentials and the local-density approximation, to study the electronic states for LEED determined structure of an ordered monolayer deposition of Sb on the InP(110) surface. A number of chemisorbed induced states have been identified in the various band gaps of InP. In particular it is found that there are three occupied and two unoccupied states in the fundamental band gap. In agreement with the inverse photoemission study of Drube and Himpsel we find that for the monolayer coverage of Sb there is no unoccupied electronic state in the fundamental band gap of InP. Charge density analysis reveals that while states localized on the second-substrate-layer atoms retain their identity, states localized on the top substrate layer atoms are changed into Sb–In and Sb–P bonding and antibonding states. In addition we identify states originating from the adsorbate layer containing the Sb–Sb chain.

1. Introduction

A detailed microscopic study of electronic states at metal–semiconductor interfaces is of fundamental interest as well as of importance in the development of sophisticated electronic devices. The atomic and electronic structures of atomically clean cleaved (110) surfaces of III–V semiconductor surfaces have been extensively studied, both theoretically (Chelikowsky and Cohen 1976, Manghi et al 1982, Srivastava et al 1983) and experimentally (Duke et al 1982, Srivastava et al 1983, Sorba et al 1987). Thus III–V(110) surfaces are ideal for investigation of metal adsorption. It has been shown by many studies that growth of a monolayer (1 ML) of group V elements Sb and Bi on clean cleaved III–V semiconductors is epitaxial, resulting in a sharp and well-defined interface with no intermixing (Stringer et al 1983, Mailhiot et al 1985, Kendelewicz et al 1989, Joyce et al 1990). This has lead to a number of experimental and theoretical studies of the III–V(110)–Sb interface with a view to understand the mechanism of Schottky barrier formation.

The two most studied interfaces are GaAs(110)–Sb and InP(110)–Sb. Experimentally, dynamical analysis of elastic low-energy electron diffraction (ELEED) intensities has been made (Duke et al 1982, 1985) to determine atomic geometry, and direct as well as inverse photoemission measurements have been presented (Stringer et al 1983, Maani et al 1985, McGovern et al 1991, Drube and Himpsel 1988) for adsorbate-induced electronic states. Theoretically, two approaches, with different degrees of sophistication, have been used to study Sb overlayers on the (110) surface of semiconductors. Self-consistent calculations, based on *local* pseudopotentials and

the X_α scheme, have been presented for electronic states on GaAs(110)–Sb (Bertoni *et al* 1983) and GaP(110)–Sb (Manghi *et al* 1987). Mailhiot *et al* (1985), on the other hand, have used an empirical sp^3s^* tight-binding model to predict the atomic geometry, chemical bonding, and surface states for an ordered monolayer of Sb on the (110) surface of GaP, GaAs, GaSb, InP, InAs and InSb. For Sb/GaAs and Sb/GaP, two systems studied by both methods, overlayer-induced states have been predicted to lie in roughly similar energy regions, but interpretation of some important states are contradictory.

As far as InP(110)–Sb is concerned, the only theoretical calculation available to-date is that by Mailhiot *et al* (1985). Their tight-binding calculation predicts one unoccupied state in the fundamental band gap, at about 1.2 eV above the valence band maximum in indium phosphide. The recent angle-resolved inverse photoemission study by Drube and Himpsel (1988), however, disagrees with the calculation of Mailhiot *et al* and predicts the lowest empty state at 2.1 eV above the valence band maximum (i.e. well above the bulk conduction band minimum). In view of the importance of InP(110)–Sb as a protypical system for an ideal metal–semiconductor interface, it is important to accurately calculate the energy locations and determine characters of Sb derived states in this system. There is another interesting reason for studying Sb on InP(110). Whereas the system GaAs(110)–Sb contains Sb–As bonds which are observed in Sb_xAs_{1-x} alloys, InP(110)–Sb offers a unique opportunity to study the nature of Sb–P bonds which are essentially unknown in either molecules or solids.

In this work we present a self-consistent calculation of electronic states and their bonding character for the InP(110)–Sb(1 ML) system. We have considered the atomic geometry as determined by the ELEED studies of Duke *et al* (1985), and have performed the calculation by using *ab-initio* non-local pseudopotentials (Bachelet *et al* 1982) and the local density approximation (LDA). A number of chemisorbed states have been found to lie in the various energy gaps of InP. Orbital characters of these states have been studied with the help of charge density plots. Our results are compared and contrasted with photoemission measurements and the theoretical work of Mailhiot *et al* (1985).

2. Details of calculation

2.1. Structural model

LEED studies show a well ordered (1 × 1) structure for room temperature deposition of 1 ML of Sb on clean cleaved InP(110) (Skeath *et al* 1980, Stringer *et al* 1983, Maani *et al* 1985, Duke *et al* 1985), with the same symmetry as the clean (110) surface. Within the (1 × 1) structure different models for adsorption of a monolayer of Sb on III–V(110) have been proposed (Skeath *et al* 1980, 1983, Duke *et al* 1982). However, dynamical ELEED studies (Duke *et al* 1982) favour a structural model in which a zig-zag chain of Sb atoms occupies the next-lattice-layer sites on the (110) surface. In this geometry the bond angle between the Sb atoms in the zig-zag chain is nearly 91°, and the surface In (P) atoms are located slightly outwards (inwards) the bulk layers. A tight-binding total-energy minimisation procedure (Mailhiot *et al* 1985) predicts that the ELEED analysis of Duke *et al* (1985) describes the atomic geometry of the InP(110)–Sb(1 ML) system quite accurately. In the present study we have, therefore, used the atomic geometry deduced from the ELEED analysis of Duke

et al (1985). A schematic diagram of the surface geometry is shown in figure 1, and a listing of the structural parameters is given in table 1. In our calculation we have ignored the uncertainties, shown in table 1 with $\pm$ signs, in the values of the various parameters. Also, note that the cation and anion positions should be interchanged when comparing figure 1 with the similar diagram in the paper by Duke *et al* (1985), or Mailhiot *et al*. In the discussion later we will represent $[\bar{1}10]$, $[001]$ and $[110]$ as x, y and z directions, respectively.
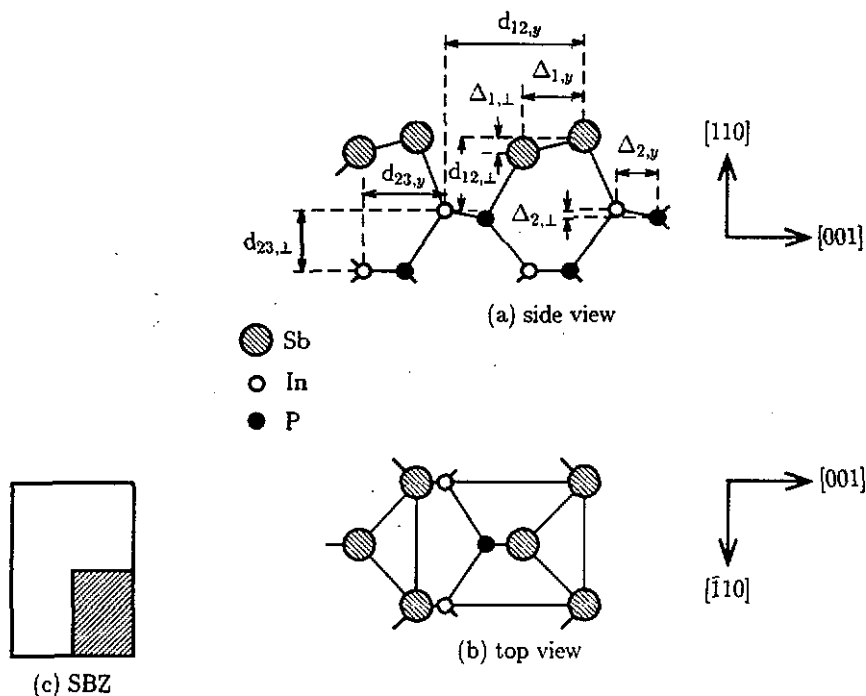

Figure 1. Schematic diagram of the surface geometry used in this work for InP(110)–Sb(1 ML). The structural parameters, determined by ELEED studies of Duke *et al*, are listed in table 1. The surface Brillouin zone, its irreducible segment, and some symmetry points are shown in (c).

2.2. Computation of electronic states

Self-consistent pseudopotential methods of calculating electronic states on clean and covered semiconductor surfaces have been extensively discussed in the literature (Schlüter *et al* 1975, Chelikowsky and Cohen 1976, Manghi *et al* 1982, Srivastava *et al* 1983). Essentially, we consider a repeated slab geometry along the surface normal and apply the usual techniques of the pseudopotential method to such an artificially generated periodic system. To study the InP(110)–Sb(1 ML) system we considered a unit cell along [110] to contain seven InP layers of the (110) surface, a Sb overlayer on each side of these layers, and five layers of vacuum. The unit cell is

orthorhombic with a volume 14 times that of the bulk primitive unit cell. The point group symmetry is C_{2v}, and the odd number of atomic planes preserves the reflection symmetry $z \longrightarrow -z$ with respect to the central plane of the slab. We considered the cubic lattice constant of InP to be the experimental value 5.869 Å.

Table 1. Structural parameters for the surface geometry of InP(110)–Sb(1 ML) displayed in figure 1, as determined by the ELEED studies of Duke *et al* (1985) and Mailhiot *et al* (1985). The cubic lattice constant of bulk InP is represented by a.

Parameter	Value (Å)
a	5.869
$\Delta_{1,\perp}$	0.70 ± 0.1
$\Delta_{1,y}$	1.98 ± 0.3
$d_{12,\perp}$	2.43 ± 0.1
$d_{12,v}$	4.46 ± 0.3
$\Delta_{2,\perp}$	0.0 ± 0.1
$\Delta_{2,y}$	1.47 ± 0.3
$d_{23,y}$	2.934

The single-particle wavefunction was expanded in symmetry adopted plane waves using the reflection symmetry $z \longrightarrow -z$. The Hamiltonian matrix was reduced to two non-zero diagonal blocks, corresponding to the even and odd combinations of the symmetry adopted basis functions. Each of the two blocks was further folded-in by using Löwdin's perturbation technique (Löwdin 1951). The size of the folded (un-folded) Hamiltonian matrix was determined by considering plane waves with kinetic energy cut-off of 5 Ryd (8 Ryd). Within the LDA the electronic eigenvalue problem was expressed in terms of the Kohn–Sham equation (Hohenberg and Kohn 1964, Kohn and Sham 1965), and the electronic exchange-correlation functional was calculated by using the scheme of Hedin and Lundqvist (1971). The norm-conserving pseudopotentials for the ions In, P, and Sb were taken from the work of Bachelet *et al* (1982). Self-consistency in the solutions of the Kohn–Sham equation was achieved by using the Broyden's convergence acceleration method (Srivastava 1984).

3. Results

In this section we present our calculated electronic eigenvalues for InP(110)–Sb(1 ML), identify some important states localized in the overlayer region, and determine characters of chemical bondings between the overlayer antimony atoms and the substrate atoms with the help of electronic charge density plots. Our interpretation of the chemical bondings will be compared and contrasted with other theoretical calculations for Sb adsorption on III–V(110) surfaces.

Before proceeding with a discussion of the results for the InP(110)–Sb(1 ML) system we remark on two issues related to the application of our theoretical scheme. One is the convergence of the equilibrium lattice constant and the convergence of the band gap with respect to the energy cut-off, and the other is the fundamental difficulty in comparing with experiments the unoccupied states derived within the LDA. To investigate the first issue we made calculations with the Hedin–Lundqvist exchange-correlation potential within the LDA and with energy cut-offs (without Löwdin's folding scheme) of 8, 10, 12 and 15 Ryd. Corresponding to these energy cut-offs the

equilibrium lattice constant values are 5.66, 5.65, 5.67 and 5.68 Å, respectively, and the direct band gap at Γ is 2.78, 2.40, 2.27 and 1.68 eV, respectively. It is clear that while a reasonably converged value of the lattice constant can be predicted from even a smaller energy cut-off of 8 Ryd, the band gap in InP would not reach a well converged value unless a much higher cut-off than 15 Ryd is used. Fully converged LDA calculations are expected to underestimate the band gap in InP, as has been well established for many semiconductors (Yin and Cohen 1982, Hybertson and Louie 1985, 1986, Godby *et al* 1988). For surface calculations, however, it would be computationally too demanding to use a reasonably large energy cut-off. It was also noticed that both increasing the energy cut-off as well as increasing the lattice constant result in a decrease in the band gap in InP. In view of these observations we chose to use a small energy cut-off and the experimental lattice constant in our calculation. Our choice of the small energy cut-off of 8 Ryd and the application of Löwdin's perturbation scheme with yet another smaller energy cut-off of 5 Ryd resulted in a band gap in InP which is somewhat bigger (about 1.9 eV) compared to the experimental value of 1.35 eV. This should be kept in mind when discussing the results, particularly unoccupied states. The second issue is more fundamental. A fully converged LDA calculation should ideally be followed by a quasi-particle calculation involving self-energy effects for a more realistic comparison of excited states between theory and experiment (Godby *et al* 1988, Hybertson and Louie 1985, 1986, 1988, Zhu *et al* 1989). Such calculations require an order of magnitude more theoretical and computational effort and have not been performed in this work. We will comment on the possible role of self-energy effects in the Sb/InP system in section 5.

In order to facilitate our study of InP(110)–Sb(1 ML) we first present a brief investigation of the electronic states on the clean InP(110) surface in its unrelaxed as well as relaxed geometries. This has been done by us in the past (Srivastava *et al* 1983), but for consistency the present calculations for InP(110) have been made by using exactly the same theoretical details as we used for studying the InP(110)–Sb system.

3.1. Clean InP(110) surface

Figure 2 shows the computed electronic eigenvalue spectrum for the InP(110) surface along the perimeter $\bar{\Gamma}\bar{X}\bar{M}\bar{X}'\bar{\Gamma}$ of the surface Brillouin zone (SBZ). The bulk energy bands projected on the (110) surface are shown by the hatched regions. We have indicated some of the commonly discussed surface states by labels A_i and C_i according to their localization at the anions (P) and cations (In), respectively.

As shown in figure 2(*a*) there are *three* sets of *true* surface states on the *unrelaxed* surface. The state A_2 is derived from the s orbital of the top layer anions (P) and for some surface wavevectors lies in the bottom of the ionicity gap of InP. The state A_5 is an occupied dangling bond band derived from the p_z orbital of the top layer anions and lies flat at about 0.4 eV above the bulk valence band maximum. The state C_3 is an unoccupied bond band derived from a mixture of s and p_z orbitals of the top layer cations (In) and lies quite flat with its lower edge near the conduction band minimum of InP.

In figure 2(*b*) are shown some of the surface states on the *relaxed* InP(110) surface. The relaxed surface geometry used in our calculation is that determined by ELEED studies and given in Kahn (1983). Compared with the unrelaxed case, there are a few noticeable changes in the energy location of some of the surface states upon relaxation. The states A_2 and A_5 are found to be most sensitive to the surface
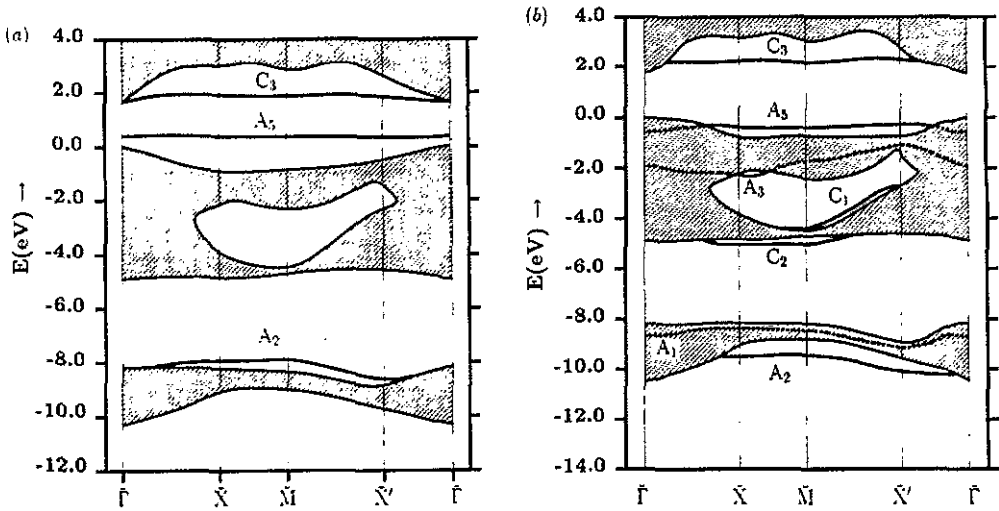
Figure 2. Energy dispersion of surface states on the InP(110) surface: (a) unrelaxed geometry, (b) relaxed geometry as determined by ELEED studies (Kahn 1983).

relaxation. Compared with previous theoretical calculations for InP(110) (Srivastava *et al* 1983, Mailhiot *et al* 1985, Alves *et al* 1991) the location of the presently calculated A_2 is at most variance: we find this state to lie below the bottom of the valence band for wavevectors along $\bar{X}\bar{M}\bar{X}'\bar{\Gamma}$. It may at first sight look puzzling, but apart from being sensitive to surface relaxation, the location of this state can also change significantly by changing the energy cut-off for the basis set in the calculation (cf Alves *et al* 1991). For the relaxed geometry the state A_5 is pushed inside the bulk valence band and at $\bar{X}$ now lies at about 0.6 eV below the valence band maximum. This compares reasonably well with the experimental result, namely 0.8 eV below the valence band maxium, reported in our previous work (Srivastava *et al* 1983). The effect of surface relaxation is to push C_3 inside the bulk conduction band, and at $\bar{X}$ it is at about 0.4 eV above the conduction band minimum. Our calculated energy gap C_3-A_5 is 2.75, 2.77, and 2.50 eV at $\bar{X}$, $\bar{M}$ and $\bar{X}'$, respectively. These values compare well with the experimental values 2.9, 3.2 and 3.1 eV at $\bar{X}$, $\bar{M}$ and $\bar{X}'$, respectively, determined from a combination of angle-resolved direct and inverse photoemission measurements (Carstensen *et al* 1990). Although not investigated for the unrelaxed geometry, we have also indicated in figure 2(b) the energy dispersion of the A_3, C_1, and C_2 surface states in some parts of the SBZ. A_3 is a p_y-like localized on the second layer P atoms. C_1 and C_2 are s-like states localized on In atoms in the second and first layers, respectively. The s-like surface state A_1, localized on P atoms in the second layer, is resonant with the bulk energy bands for wavevectors throughout the SBZ. In figure 3 we have displayed the characters of the states A_1, A_2, A_3, A_5, C_1, C_2 and C_3 through charge density plots.

3.2. InP(110)-Sb(1 ML)

For a monolayer deposition of Sb on the InP(110) surface we used the ELEED geometry as discussed in section 2. Before discussing the energy location and bonding
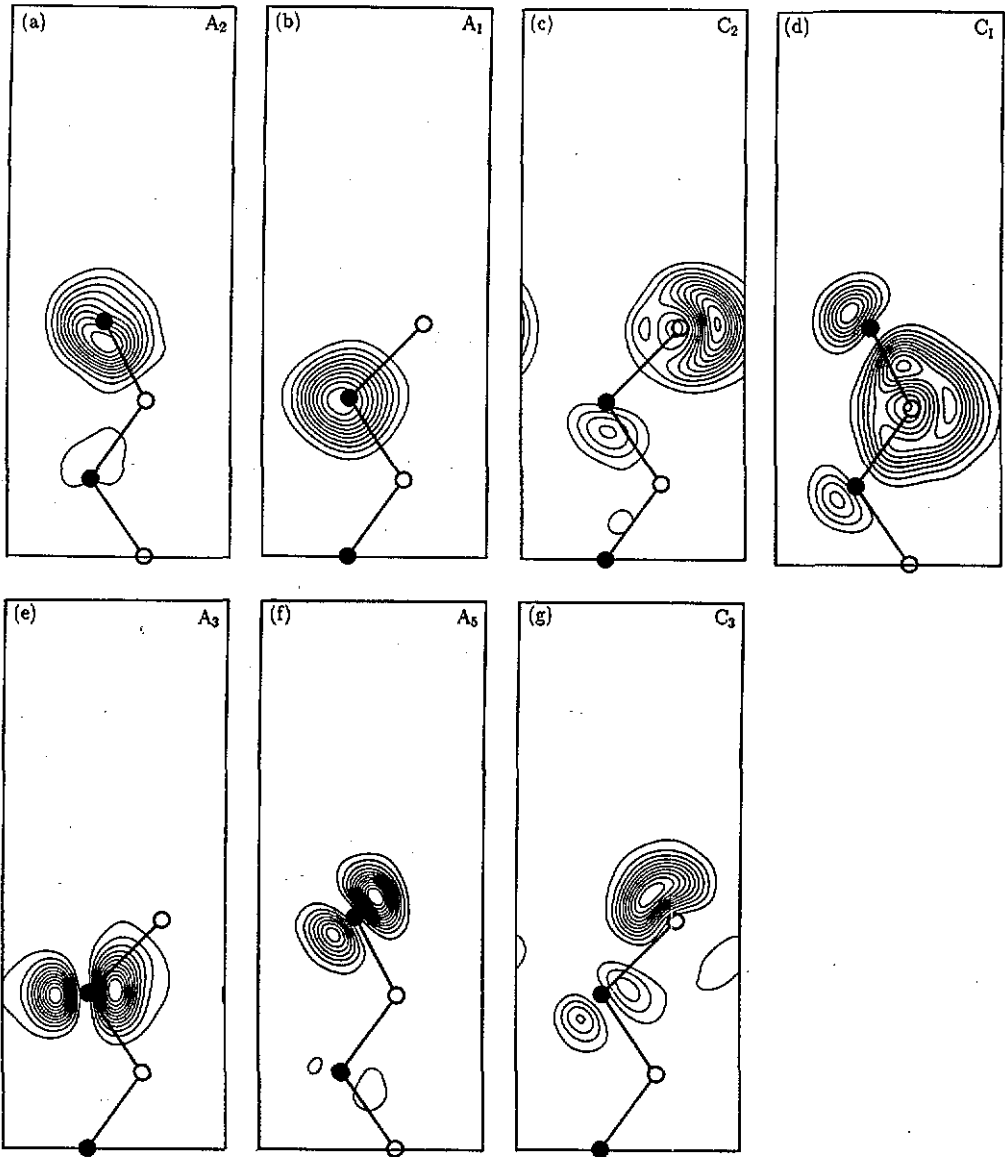
Figure 3. Electronic charge density contour plots for individual surface states for the relaxed geometry of the InP(110) surface: (*a*) A_2 at $\bar{X}$, (*b*) A_1 at Γ; (*c*) C_2 at $\bar{X}$, (*d*) C_1 at $\bar{M}$; (*e*) A_3 at $\bar{X}$; (*f*) A_5 at $\bar{X}'$; (*g*) C_3 at $\bar{X}$.

character of individual electronic states, we first make some observations about the electronic charge density summed over all occupied states. Figures 4(*a*) and 4(*b*) show the total charge density plots in the y–z planes containing the Sb–In and Sb–P bonds, respectively. For comparison we have also shown, in figures 4(*c*) and 4(*d*), the total charge density plots for the clean surface with the chains terminating at In and P, respectively. The first feature to note is that both on the clean as well as the covered surface the charge heals up at the top layer, with no leakage in the vacuum region. It is also clear that the overlayer Sb atoms are linked to the sustrate by

directional bonds. The bonding between Sb and In is covalent, with partial ionicity as expected in the semiconductor InSb. The In–Sb bond is seen to be weaker than the substrate In–P bond. The charge density around the P atoms on the top surafce layer has changed significantly: the healing of the occupied dangling bond charge on these atoms has been changed into a strong covalent bonding between Sb and P. This bond shows a slight ionicity, with Sb and P playing the roles of cation and anion, respectively. This is due to the fact that P is more electronegative than Sb. The bond Sb–P is shorter than the bond In–P and shows a larger concentration of charge. Thus the overlayer Sb atoms show two different types of bonding with the substrate: Sb atoms bonded to the substrate In(P) atoms behave as anions(cations).

In figure 5(a) the charge density in a tilted surface plane which contains the Sb–Sb chain is shown. Clearly the bonding between two neighbouring Sb atoms in the chain is covalent. The double humped feature of this covalent bonding is driven by the relaxation of the overlayer: the Sb–Sb and Sb–In distances are about 11% longer, and the Sb–P distance is about 18% shorter, than the bulk In–P bond length. This was verified by comparing this plot with a similar plot with Sb atoms at the ideal zincblende atomic positions, which showed one broad maximum midway between the two neighbouring Sb atoms. The Sb atom which bonds with the P atom in the top substrate layer shows a pronounced strengthening of charge in the back bonding direction. This is actually a projection on the tilted horizontal plane of the covalent bonding between Sb and P. This point is better appreciated in figure 5(b) which shows the Sb–Sb bond, along with a projection of the Sb–P bond, in a vertical plane. Also shown in the same figure are the third and fifth atomic layers containing the In–P bonds. Also, the charge density distribution in figure 5(b) provides an evidence of π bonding in the Sb chain.

Now we will discuss the energy dispersion and localization of individual electronic states on InP(110)–Sb(1 ML). The surface and chemisorbed-induced states along the perimeter $\bar{\Gamma}\bar{X}\bar{M}\bar{X}'\bar{\Gamma}$ of the SBZ are plotted in figure 6. We have mostly focused on the states in the bulk band gaps. The states labelled A_i, C_i and S_i are derived from the substrate anion (P), substrate cation (In), and the overlayer (Sb) atoms, respectively. For clarity we will divide the discussion of these states in three energy groups.

3.2.1. States in the ionicity gap and below. As seen in figure 2(b) there are three states (A_1, A_2, C_2) localized on the clean InP(110) surface with energies below the upper edge of the ionicity gap. For the InP(110)–Sb(1 ML) system we find a total of five states in this energy range.

The state localized on the surface phosphorus atoms, A_2, has been replaced by the state S_1 which lies well below the bottom of the valence band. As is clearly seen in figure 7(a), it is an ssσ bonding state between the overlayer Sb atoms and the substrate P atoms. A similar observation has been made for Sb/GaP by Manghi *et al* (1987) (their state S_1'). The state A_1, which is localized on the second substrate phophorus atoms (figure 7(b)), retains its orbital character but is pushed down in energy and now resonates with the lower part of the valence band. The state labelled S_2 is localized on Sb atoms bonded to substrate In atoms, as shown in figure 7(c)) and lies in the bottom of the ionic gap along $\bar{X}$–$\bar{M}$. The state S_3 can be described as an antibonding ssσ state between Sb atoms and substrate P atoms (figure 7(d)). Thus it is an antibonding partner of S_1. This state is similar to that observed on Sb/GaP by Manghi *et al* (1987) (their state S_2). Just below the upper edge of the ionic gap
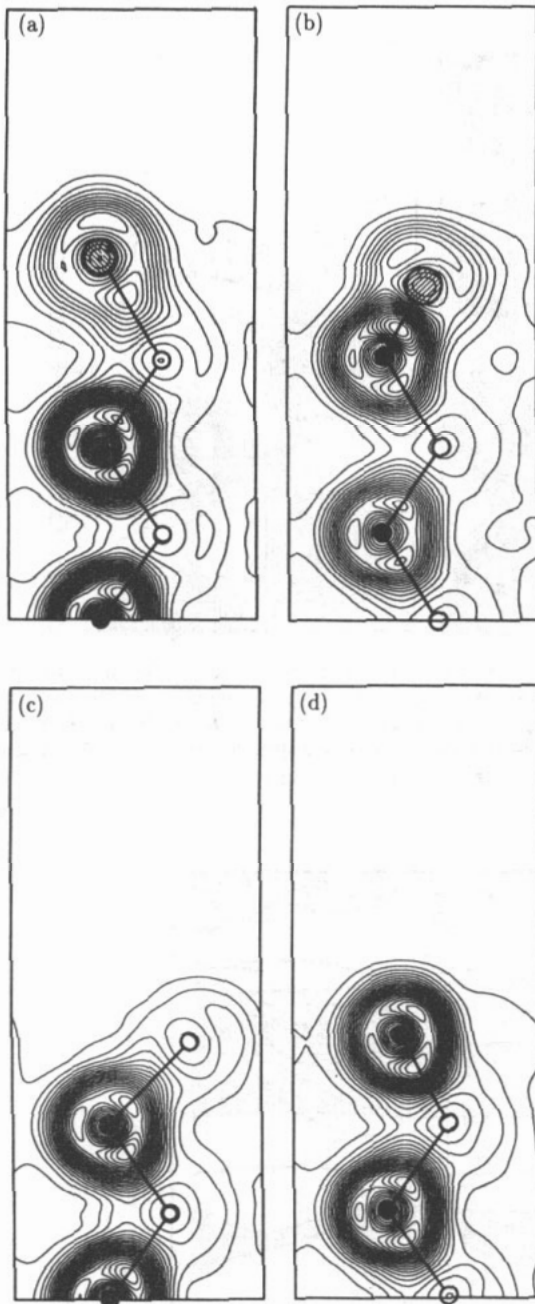
Figure 4. Total valence charge density contours for InP(110)–Sb(1 ML) plotted in ($\bar{1}$10) planes containing the: (*a*) Sb–In bond and (*b*) the Sb–P bond. Also shown for comparison are plots for the clean relaxed InP(110) surface in ($\bar{1}$10) planes passing through (*c*) In and (*d*) P surface atoms.

we observe the state S_4 along $\bar{X}$–$\bar{M}$–$\bar{X}'$. This is another $ss\sigma$-like state contributed by bonding between Sb atoms and substrate In atoms (figure 7(*e*)). Thus this is a
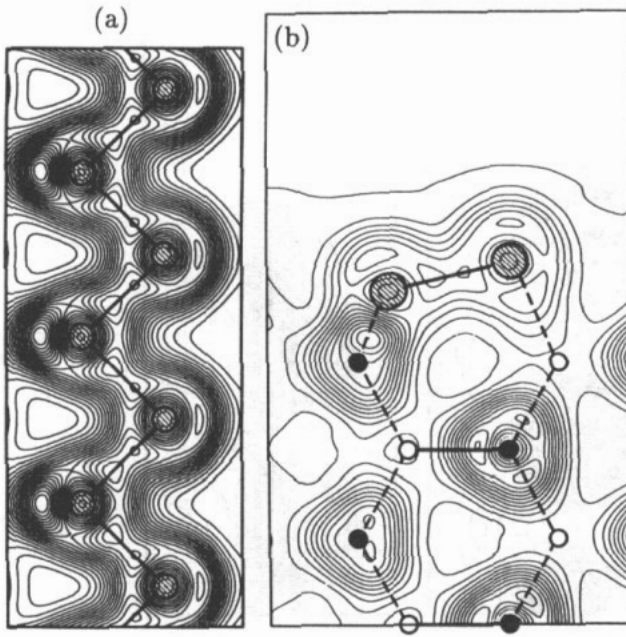
Figure 5. Contours of the total valence charge density for InP(110)–Sb(1 ML) plotted in (a) a tilted horizontal (110) plane containing the chain of Sb atoms; and (b) a vertical plane containing a Sb–Sb bond. Also shown in (b) are the third and fifth atomic layers containing the In–P bonds. The charge distribution in (b) provides evidence of π-bonding between neighbouring atoms in the Sb chain.
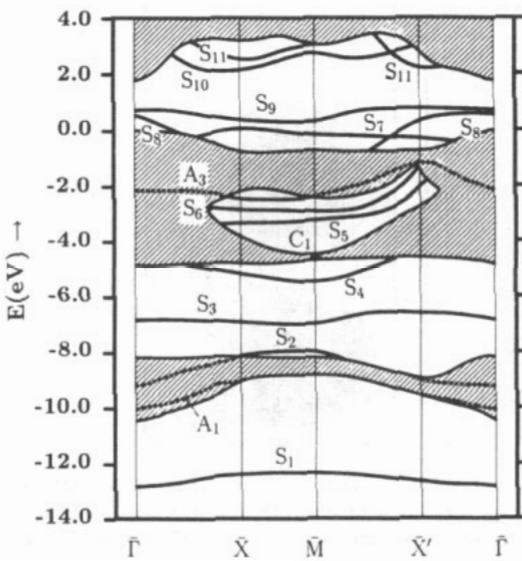

Figure 6. Energy dispersion of surface and chemisorbed-induced electronic states on InP(110)–Sb(1 ML). The atomic geometry used in the calculation is taken from the ELEED studies of Duke *et al* (1985).
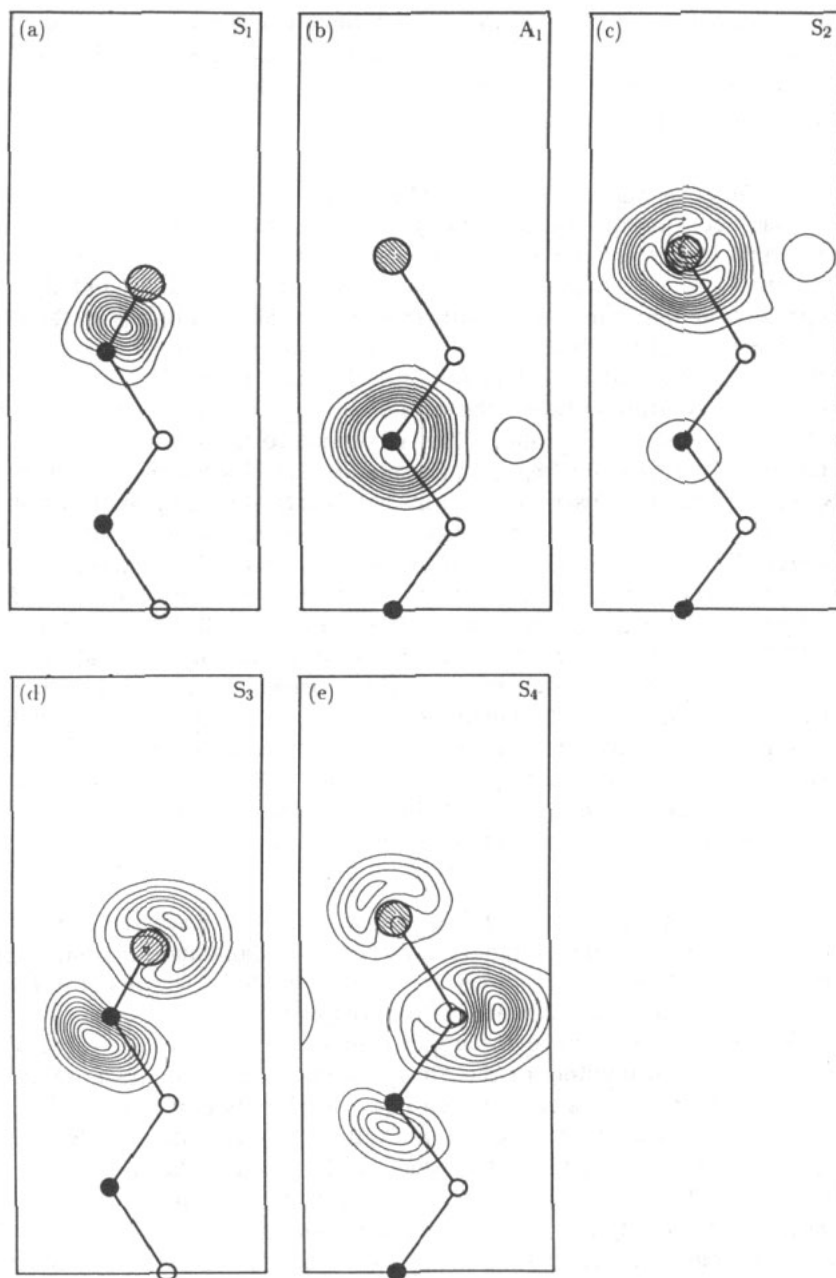
Figure 7. Charge density distribution of individual states on InP(110)–Sb(1 ML): (*a*) S_1 at $\bar{M}$; (*b*) A_1 at $\bar{X}$; (*c*) S_2 at $\bar{X}$; (*d*) S_3 at $\bar{M}$; (*e*) S_4 at $\bar{X}$.

replacement for the C_2 state on the clean surface.

The results obtained from our calculations are in sharp contrast with the picture presented by the tight-binding method of Mailhiot *et al*. According to these authors the state lying below the valence band minimum is A_1. Their work predicts two

occupied overlayer states in the energy range considered here. These states (S_1 and S_2 in their notation) correspond to the non-bonding symmetric and anti-symmetric s-like lone pairs within the Sb chain. Their work does not discuss the status of A_2 upon chemisorption.

3.2.2. States in the stomach gap. The surface state C_1 remains largely unmodified, but has been pushed down in energy and now resonates with bulk bands. We have identified this state only at $\bar{M}$ with its location shown in figure 8(*a*). In the stomach gap there are two chemisorbed-induced states, labelled S_5 and S_6. The state S_5 represents bonding between a superposition of Sb p_x orbitals in the overlayer chain and the p_y atomic orbital of the substrate P atoms. This agrees with the observation made by Manghi *et al* (1987) for Sb/GaP (their state S_3'). The state S_6, similarly, represents bonding between the orbital $p_x p_x \sigma$ in the Sb chain and the p_z atomic orbital of substrate P atoms. This is similar to a stomach gap state identified by Bertoni *et al* (1983) for Sb/GaAs (their state S_3). These observations about the states S_5 and S_6 can be clearly made from the charge density plots given in figures 8(*b*)–(*e*). The state A_3 is slightly pushed down in energy but otherwise has the same overall dispersive behaviour as on the clean surface. The charge density plot, given in figure 8(*f*), shows that A_3 retains its feature and can be compared with the plot in figure 3(*e*) for the clean surface. The works of Mailhiot *et al* (1985), Bertoni *et al* (1983), and Manghi *et al* (1987) do not seem to identify this feature of the state A_3.

On the whole our interpretation of the origin of stomach gap states is similar to that of Bertoni *et al* and Manghi *et al* (1987), but disagrees with Mailhiot *et al* who consider these states to be associated predominantly with the p^2-bonding states of the plane of the overlayer Sb chain. A fully self-consistent calculation and careful analysis of charge density plots in different planes has allowed us to obtain a better understanding of the characters of individual states.

3.2.3. States in the fundamental band gap. Now we discuss the electronic states in the most important energy range, namely the fundamental bulk band gap region. We have identified five states, which are labelled S_7–S_{11}. The first three of these states are occupied and the other two are unoccupied.

The state S_7 lies above the upper edge of the bulk valence band along $\bar{X}$–$\bar{M}$–$\bar{X}'$ and results from bonding of the Sb p_z orbital with the dangling bond orbital of the substrate In atom. This can be seen from the density plot in figure 9(*a*). Such a state has also been found on Sb/GaAs as well as Sb/GaP (state S_6 Bertoni *et al* (1983) and Manghi *et al* (1987)). The state S_8 is found to lie above the upper valence band edge along $\bar{\Gamma}$–$\bar{X}$ and along $\bar{\Gamma}$–$\bar{X}'$. We find this to be a $pp\sigma$-like state on the plane of the Sb atoms, with its charge density given in figure 9(*b*). This state has some resemblance with a state along $\bar{\Gamma}$–$\bar{X}'$ for Sb/GaP (the state S_4' in Manghi *et al* (1987)). The top most occupied state, S_9 appears to result from bonding between Sb sp_z and P p_z orbitals, with its charge density given in figure 9(*c*). This state shows an energy dispersion of about 0.4 eV, with its upper edge at about 0.85 eV above the bulk valence band maximum.

Our interpretation of the states S_7 and S_9 is somewhat similar to that presented by Mailhiot *et al* (1985) who associated the chemisorbed induced occupied states in the band gap (their states S_5 and S_6) to bonding between substrate dangling bond and π-electron orbitals (made of p_z orbitals) normal to the plane of the Sb chain.
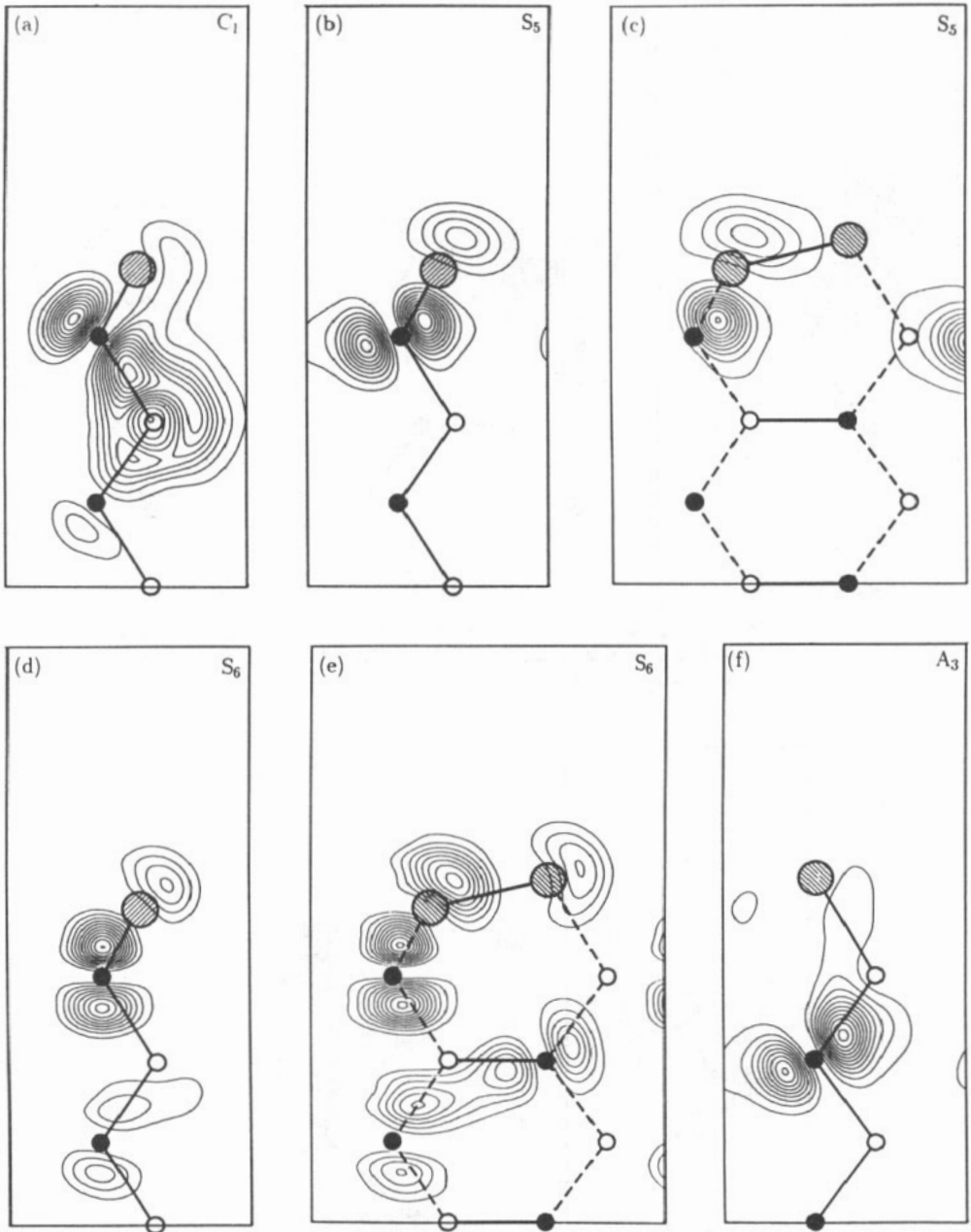
Figure 8. Charge density distribution of states on InP(110)–Sb(1 ML) falling in the stomach gap: (a) C_1 at $\bar{M}$; (b) S_5 at $\bar{X}$; (c) S_5 at $\bar{X}$ in a vertical plane containing the Sb–Sb bond; (d) S_6 at $\bar{X}'$; (e) S_6 at $\bar{X}'$ in a vertical plane containing the Sb–Sb bond; (f) A_3 at $\bar{X}$.

In our work an evidence of π-bonding normal to the plane of the Sb chain can be seen from the total charge density plot presented in figure 5(b).
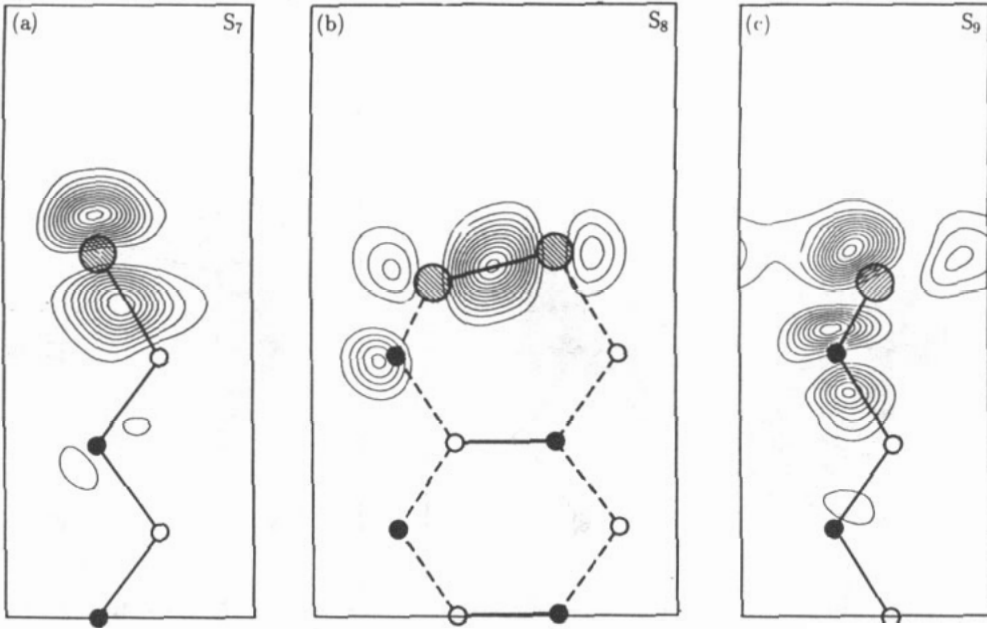
Figure 9. Charge density distribution of occupied states on InP(110)–Sb(1 ML) lying in the fundamental band gap: (a) S_7 at $\bar{X}'$; (b) S_8 at $\bar{\Gamma}$ in a vertical plane containing the Sb–Sb bond; (c) S_9 at $\bar{M}$.
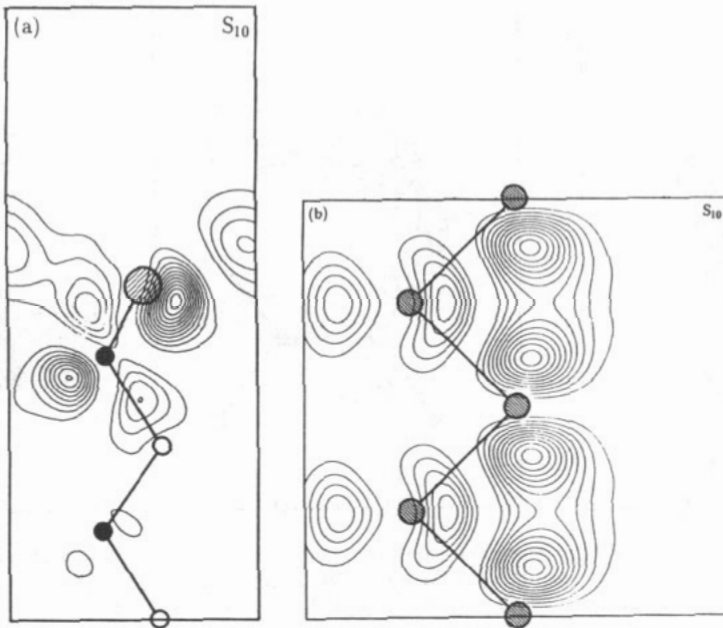

Figure 10. Charge density distribution of the unoccupied state S_{10} on InP(110)–Sb(1 ML): (a) at $\bar{X}$ in a $(\bar{1}10)$ plane; (b) at $\bar{X}$ in a tilted horizontal plane containing the chain of Sb atoms.

Figures 10(a) and (b) show charge density plots for the state S_{10}. From figure 10(b) it is clear that this state is made from p_x and p_y orbitals of the Sb chain. There is also evidence of overlap between p_y orbitals from next-nearest Sb atoms on the plane. From figure 10(a) it is clear that there is an antibonding coupling between Sb p and P p orbitals. Thus we conclude that the state S_{10} represents an antibonding coupling between Sb and P electrons, with a large contribution from empty Sb p orbitals. This state can be compared with a low lying chemisorbed-induced unoccupied state on Sb/GaAs (state S_7 in Bertoni *et al* (1983)) and on Sb/GaP (state S_8 in Manghi *et al* (1987)). This state may further be considered as the antibonding counterpart of the state S_5. The character of the state S_{11} can be deduced from the charge density plots in figures 11(a) and (b). On the overlayer it has the same character as S_{10}, but with the positions of p_x and p_y orbitals swapped between the two basis Sb atoms. From figure 11(a) it appears to be a state resulting from an antibonding coupling between Sb and In, with a large contribution from empty Sb p orbitals. This state can also be compared with a low lying chemisorbed unoccupied state on Sb/GaAs (state S_8 in Bertoni *et al* 1983) and Sb/GaP (state S_7 in Manghi *et al* (1987)).
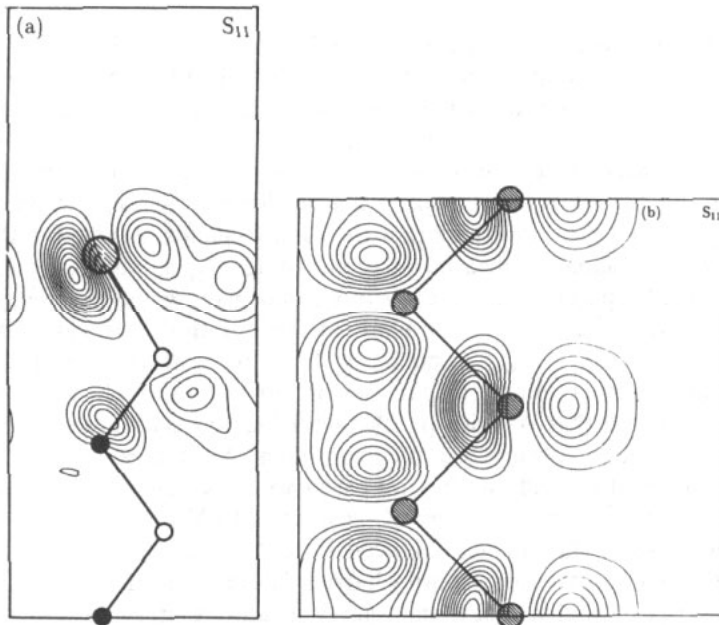

Figure 11. Charge density distribution of the unoccupied state S_{11} on InP(110)–Sb(1 ML): (a) at $\bar{X}$ in a $(\bar{1}10)$ plane; (b) at $\bar{X}$ in a tilted horizontal plane containing the chain of Sb atoms.

Our interpretation of the empty states S_{10} and S_{11} differs from that of Mailhiot *et al* (1985) who have suggested the corresponding states (their states S_7 and S_8) as π-antibonding (made from p_z orbitals) normal to the plane of the Sb chain.

4. Comment on LEED geometries for the clean and Sb covered InP(110) surfaces

For the LEED geometries used in the present investigation of the electronic states on the clean and Sb covered InP(110) surfaces we have also calculated Hellmann–

Feynman forces (see e.g. Ihm *et al* 1979) on surface atoms. We find that the forces on the clean surface atoms are small, indicating that the LEED geometry for InP(110) is near the minimum energy configuration. The LEED geometry we have used is characterized by a tilt of 28.1° of the surface atomic layer on InP(110). The structural parameters of this geometry agree quite well with the recent *ab-initio* theoretical predictions by Alves *et al* (1991).

For InP(110)–Sb(1 ML), however, the LEED atomic geometry of Duke *et al* (1985) leaves significantly large forces on the overlayer Sb atoms as well as P atoms on the top substrate layer. An analysis of computed forces indicates that to reach the minimum energy configuration the LEED geometry should be refined to accommodate (i) a somewhat larger P–Sb bond length, and (ii) a smaller vertical corrugation of the Sb overlayer. An attempt to determine equilibrium geometry is in progress. It is hoped, however, that a good deal of physics has already emerged from the results obtained with the LEED geometry.

5. Comparison with photoemission studies

An investigation of occupied surface electronic states of the InP(110)–Sb(1 ML) system by angle-resolved photoemission spectroscopy has recently been reported (McGovern *et al* 1991). In this section we make a preliminary attempt to compare our theoretical results with the experiment. In an energy range of about 6 eV below the highest occupied state these authors have identified four surface- or overlayer-related bands along $\bar{X}'-\bar{\Gamma}-\bar{X}$. It is clear from figure 6 that in this energy range we have identified a total of eight such states. We think that the top two bands obtained in the experiment can be tentatively assigned to a mixer of the states S_7, S_8 and S_9 in figure 6, which are either closely spaced or cross each other and may not be easily separable in the experiment. The third band in the work of these authors can similarly be assigned to a mixer of the states A_3, S_6 and S_5 in figure 6, as all of these are within about 1 eV and show similar energy dispersion for most of the surface Brillouin zone. It should be remarked that A_3 with p_y character has low photoionisation cross section and may not be clearly observed in the experiment (Srivastava *et al* 1983). The fourth photoelectron surface band can be compared with the state S_4 in figure 6, although we have in addition identified S_3 which lies about 1 eV below S_4.

The lowest lying chemisorbed-induced state, S_{10}, could prove to be most important from the point of view of Schottky barrier formation at the Sb/InP(110) interface. Therefore it is essential to know the energy location of this state in relation to the conduction band edge in bulk InP. Our calculation suggests that both the states S_{10} and S_{11} show large dispersion, with the lowest energy of S_{10} being about 0.4 eV above the conduction band minimum in InP. It should be reiterated that, due to combined effects of the LDA and Löwdin's perturbation technique for matrix diagonalization with a small energy cut-off, the calculated conduction band energies are somewhat inaccurately predicted. Nevertheless, we expect that their relative positions are correctly reproduced. We thus conclude that there are no chemisorbed-induced unoccupied gap states for a monolayer deposition of Sb on InP(110). This conclusion is in disagreement with the theoretical results of Mailhiot *et al* who found a flat unoccupied state lying below the bulk conduction band edge. Our conclusion, on the other hand, receives support from the inverse photoemission measurement of Drube and Himpsel (1988), according to which the lowest unoccupied Sb-induced state on

InP(110) lies at 0.75 eV above the bulk conduction band edge. The dispersion trend for S_{10} obtained in this work, however, disagrees with their inverse photoemission measurement. We find a downward dispersion of S_{10} from $\bar{\Gamma}$ towards $\bar{X}$, whereas the opposite trend is observed in the measurement.

It is important to remark on the discrepancies between the theoretical and experimental results for the unoccupied state S_{10}. In this connection it is interesting to note that the recent work of Zhu *et al* (1989) has highlighted similar discrepancies between theory and experiment regarding the location and dispersion of unoccupied states on the clean GaAs(110) surface. The state-of-the-art quasi-particle calculation by Zhu *et al* predicts the energy location and dispersion of the lowest unoccupied surface state in complete contrast to some inverse photoemission measurements. The work of Zhu *et al* has also highlighted significant discrepancies between different inverse photoemission measurements. Regarding the theoretical prediction of the S_{10} state for the Sb/InP system, its location and dispersion are likely to change with (i) higher energy cut-off, (ii) different atomic relaxation at the interface, and (iii) inclusion of self-energy effects. The work of Zhu *et al* clearly demonstrates that the effect of the self-energy is mainly to raise the unoccupied surface state energies by nearly a constant shift, and to decrease the occupied surface state energies by a much smaller amount. We expect a similar role of the self-energy effects in the Sb/InP system. As discussed earlier the effect of a higher energy cut-off will be to lower the energy location of all unoccupied states, but otherwise we do not expect the dispersion of the state S_{10} to change appreciably. We did not try different atomic geometries at the interface to study any likely changes in the dispersion of S_{10}. In any case we believe that while a fully converged calculation may somewhat change the energy position of the state S_{10}, the discrepancies regarding its dispersion between the theory and the inverse photoemission results are beyond the inadequacy of the present calculation.

6. Summary

A self-consistent pseudopotential calculation has been made for the electronic band structure of the InP(110)–Sb(1 ML) system using the LEED atomic geometry. It has been found that deposition of an ordered monolayer of Sb on the InP(110) surface results in the following situation regarding electronic states.

(i) There is virtually no alteration of orbital characters of the states localized on the second layer substrate atoms (namely states A_1, C_1 and A_3);

(ii) the states localized on the top surface layer atoms (namely A_2, C_2, A_5 and C_3) have been converted into overlayer-substrate (namely Sb–In and Sb–P) bonding states, and

(iii) some gap states are characterized by bonding between Sb–Sb intrachain and substrate dangling bond orbitals.

Apart from the unremoved surface states on the second layer surface atoms, we have identified a total of eleven chemisorbed-induced states in the various band gaps of InP, nine of which are occupied. A preliminary comparison of our results with direct and inverse photoemission measurements is encouraging but a more detailed comparison is warranted. In particular, it is found that, in agreement with the inverse photoemission studies of Drube and Himpsel, the lowest unoccupied chemisorbed-induced state lies above the conduction band minimum in InP. Finally, it is remarked

that the LEED geometry does not represent a totally acceptable minimum energy configuration for InP(110)–Sb(1 ML) and a finer optimization of the structural parameters should be undertaken.

Acknowledgments

References

Alves J L, Hebenstreit J and Scheffler M 1991 *Phys. Rev.* B **44** 6188
Bachelet G B, Hamann D R and Schlüter M 1982 *Phys. Rev.* B **26** 4199
Bertoni C M, Calandra C, Manghi F and Molinari E 1983 *Phys. Rev.* B **27** 1251
Carstensen H, Claessen R, Manzke R and Skibowski M 1990 *Phys. Rev.* B **41** 9880
Chelikowsky J R and Cohen M L 1976 *Phys. Rev.* B **13** 826
Drube W and Himpsel F J 1988 *Phys. Rev.* B **37** 855
Duke C B, Mailhiot C, Paton A, Li K, Bonapace C and Kahn A 1985 *Surf. Sci.* **163** 391
Duke C B, Paton A, Ford W K, Kahn A and Carelli J 1982 *Phys. Rev.* B **26** 803
Godby R W, Schlüter M and Sham L J 1988 *Phys. Rev.* B **37** 10159
Hedin L and Lundqvist B I 1971 *J. Phys. C: Solid State Phys.* **4** 2064
Hohenberg P and Kohn W 1964 *Phys. Rev.* B **136** 864
Hybertson M S and Louie S G 1985 *Phys. Rev. Lett.* **55** 1418
—— 1986 *Phys. Rev.* B **34** 5390
—— 1988 *Phys. Rev.* B **38** 4033
Ihm J, Zunger A and Cohen M L 1979 *J. Phys. C: Solid State Phys.* **12** 4409
Joyce J J, Nelson M M, Tang M, Meng Y, Anderson J and Lapeyre G J 1990 *J. Vac. Sci. Technol.* A **8** 3542
Kahn A 1983 *J. Vac. Sci. Technol.* A **1** 684
Kohn W and J L Sham 1965 *Phys. Rev.* A **140** 1133
Kendelewicz T, Miyano K, Cao R, Lindau I and Spicer W E 1989 *J. Vac. Sci. Technol.* B **7** 994
Löwdin P-O 1951 *J. Chem. Phys.* **19** 1396
Maani C, McKinley A and Williams R H 1985 *J. Phys. C: Solid State Phys.* **18** 4975
Mailhiot C, Duke C B and Chadi D J 1985 *Phys. Rev.* B **31** 2213
Manghi F, Calandra C and Molinari E 1987 *Surf. Sci.* **184** 449
Manghi F, Molinari E, Bertoni C M and Calandra C 1982 *J. Phys. C: Solid State Phys.* **15** 1099
McGovern I T, Whittle R, Zahn D R T, Muller C, Nowak C, Cafolla A and Braun W 1991 *J. Phys.: Condens. Matter* **3** SA 367
Schlüter M, Chelikowsky J R, Louie S and Cohen M L 1975 *Phys. Rev.* B **12** 4200
Skeath P, Su C Y, Lindau I and Spicer W E 1980 *J. Vac. Sci. Technol.* **17** 874
Skeath P, Su C Y, Harrison W A, Lindau I and Spicer W E 1983 *Phys. Rev.* B **27** 6246
Sorba L, Hinkel V, Middelmann H U and Horn K 1987 *Phys. Rev.* B **36** 8075
Srivastava G P 1984 *J. Phys. A: Math. Gen.* **17** L317
Srivastava G P, Singh I, Montgomery V and Williams R H 1983 *J. Phys. C: Solid State Phys.* **16** 3627
Stringer C, McKinley A, Hughes G and Williams R H 1983 *Vacuum* **33** 597
Yin M T and Cohen M L 1982 *Phys. Rev.* B **26** 5668
Zhu X, Zhang S B, Louie S G and Cohen M L 1989 *Phys. Rev. Lett.* **63** 2112